buildings

MDPI

Article

Dynamic Analysis of a Steel–Concrete Composite Box-Girder Bridge–Train Coupling System Considering Slip, Shear-Lag and Time-Dependent Effects

Ce Gao [1,2], Li Zhu [1,*], Bing Han [1], Qing-Chen Tang [1] and Rui Su [1]

[1] School of Civil Engineering, Beijing Jiaotong University, Beijing 100044, China
[2] China Railway Economic and Planning Research Institute Co., Ltd., Beijing 100038, China
* Correspondence: zhuli@bjtu.edu.cn

Abstract: A dynamic computational program considering slip, shear-lag and time-dependent effects of composite box-girder bridge–train coupling system is firstly proposed based on the authors' previous studies. In the program, the long-term vertical displacement of a composite bridge is firstly calculated. The calculated vertical displacement is then superimposed on the existing uneven track as the new excitation of the composite box-girder bridge–train coupling system to obtain the dynamic responses of the bridge–train coupling system. A 3 × 40 m simply supported steel–concrete composite box-girder bridge is selected to investigate the influence of its time-dependent behavior on its dynamic responses. The results showed that the time-dependent effect will amplify the dynamic characteristics of the composite box-girder bridge and the high-speed train. The maximum vertical displacement and acceleration of the composite bridge increase by 8.82% and 13.64%, and the maximum vertical acceleration of the train body increases by 144.78%. Additionally, the slip and shear-lag effects have an impact on the dynamic responses of the composite box-girder bridge–train coupling system at different operation times. The dynamic responses of the coupling system strengthen with the decrease in shear connection stiffness. The dynamic responses of the system may be underestimated when the shear-lag effect is not neglected. Therefore, these conclusions should be given sufficient attention in the design, construction and operation of high-speed railway composite bridges.

Keywords: steel-concrete composite box-girder bridge-train coupling systems; time-dependent effect; dynamic characteristics; slip; shear lag

Citation: Gao, C.; Zhu, L.; Han, B.; Tang, Q.-C.; Su, R. Dynamic Analysis of a Steel–Concrete Composite Box-Girder Bridge–Train Coupling System Considering Slip, Shear-Lag and Time-Dependent Effects. *Buildings* **2022**, *12*, 1389. https://doi.org/10.3390/buildings12091389

Academic Editors: Jiaji Wang, Xin Nie, He Zhao and Yingjie Zhu

Received: 8 August 2022
Accepted: 1 September 2022
Published: 5 September 2022

1. Introduction

Steel-concrete composite box-girder bridges are increasingly and widely utilized as a new type of bridge structure because they can fully utilize the compressive strength of concrete slabs and the tensile strength of steel beams. The steel-concrete composite box-girder bridge is called a 'thin-walled structure', and is composed of several kinds of materials. The special composition and section characteristics of steel-concrete composite girder bridges determine their special mechanical characteristics, namely, the slip effect and shear lag effect, which differ from other structures.

The shrinkage and creep of concrete will impact the long-term performance of steel-concrete composite box-girder bridges. Therefore, the mechanical characteristics of composite girders will be more complicated under the comprehensive influence of the time-dependent slip and shear lag effects. Many studies have examined the calculation method of the time-dependent characteristics of composite girder bridges due to the shrinkage and creep influence of concrete material [1–4]. In light of the shrinkage influence, the concrete shrinkage strain changes independently of its stress state, so during the course of the calculation, the initial strain can be applied to a structure, and the treatment method is simpler. However, for the creep influence, because the creep strain of concrete is related to the stress state, not only at its current state but also through the whole stress history,

its calculation is more complicated. The general step method and single-step algebraic method are commonly used to investigate the creep behavior of structures. Single-step algebraic methods, such as the effective modulus method (EM) [1], mean stress method (MS) [2], and effective modulus method adjusted by age (AAEM) [3], are employed to handle numerical integrals by various quadratic formulas, where the stress history can be disregarded, but this will affect the accuracy of the solution. Bazant [4] proposed a general step-by-step calculation method to solve numerical integration with the mid-point rule and trapezoidal rule in numerical integration. Zhu and Su [5] compared the solution results of the model using the general step method and single-step algebraic method and discovered that the single-step algebraic method could make a good prediction of the time-dependent characteristics of the composite beam, except for the shear warpage displacement of the simply supported composite beam. Gilbert and Bradford [6] tested a long-term performance of two two-span, continuous composite beams for 340 days and pointed out that the time-dependent effect of concrete has a significant impact on the mechanical characteristics of continuous composite beams, and three main methods were employed to analyze the sliding effect: methods based on finite element theory, methods based on built-in degrees of freedom [7] and methods based on spring elements [8]. These methods are used to simulate the sliding effect between the concrete slab and the steel box. The study of steel-concrete composite beams started to consider the sliding effect [9–11]. An analytical method [12,13] was used to establish the control equation of steel-concrete composite beams considering the sliding effect. Research on the shear lag influence of steel-concrete composite girder bridges mainly adopts the analytical solution method [14,15] and numerical calculation method [16–20].

Current research on the dynamic responses of bridge–train coupling systems is largely concentrated on perfecting the vehicle model. In the established train model, the spring mass [21], harmonic load [22], moving mass [23] and multirigid spring-damping system [24–28] are utilized to simulate the dynamic action of a vehicle. In view of the research on steel-concrete composite box-girder bridge–vehicle coupling systems, scholars from various countries have made preliminary explorations. Zhou et al. [29] established the governing differential equation of a steel-concrete composite box-girder considering the shear lag effect, slip and moment of inertia through the Hamilton principle and deduced the natural frequency equation of a steel-concrete composite box-girder with distinct boundaries on the basis of corresponding boundary conditions. To analyze the law governing the influence of the slip effect on the dynamic response of the steel-concrete composite beam-vehicle coupling system, Wang and Zhu [30] proposed an analytical model for a steel-concrete composite beam–vehicle coupling system considering the slip effect using beam elements to establish the concrete slab and the steel box beam structure connected by shear connectors simulated as vertical horizontal springs. Uiker-Kaustell and Karoumi [31] applied the theory of continuous wavelet transform to study the amplitude correlation between the natural vibration frequency of the first-order mode-vertical bending and the equivalent viscous mode damping ratio of a railway steel-concrete composite beam bridge along with a single span ballastway bridge deck. Liu et al. [32] analyzed the dynamic evaluation and modeling of a vehicle–bridge coupling system of steel-concrete composite beams by selecting steel-concrete composite beams (taking into account four steel plate beams) and steel-concrete composite box beams as research objects. Zhu et al. [33] derived the vibration equation of a steel-concrete composite beam-vehicle coupling system based on finite element theory, Euler-Bernoulli beam theory and the virtual work principle, solved it by the Newmark-β method, and analyzed slip and shear lag effects on the dynamic responses of steel-concrete composite beams and trains. All the above reveal that current studies about the dynamic characteristics of the steel-concrete composite girder bridge–vehicle coupling system mainly focus on the free vibration characteristics or transient dynamic characteristics, and the influence of the time-dependent effect on them has not been further explored. Therefore, the dynamic characteristics of the steel-concrete composite box-girder

bridge under self-excitation of the train considering the time-dependent effect need to be further analyzed.

This study proposes a computation program of the dynamic characteristics of a composite box-girder bridge–train coupling system considering shear lag, interface slip and time-dependent effects. Based on the program, the dynamic characteristics of the composite box-girder-train coupling system are analyzed, and a parametric analysis is conducted. The novelty of the study is to investigate the influence of long-term deflection on the dynamic responses of a composite box-girder bridge–train coupling system based on a proposed dynamic analysis model of composite box-girder bridge–train coupling system which can elaborately simulate the spatial mechanical behavior of composite box-girder bridges.

2. Influence of the Time-Dependent Behavior on the Dynamic Characteristics of the Composite Box-Girder Bridge–Train Coupling System

2.1. Brief Introduction of the Dynamic Analysis Model Considering Slip, Shear-Lag and Time-Dependent Effects

A dynamic computational program considering the slip, shear-lag and time-dependent effects of composite box-girder bridge–train coupling systems consists of two models: (1) a time-dependent analysis model of composite beams considering the slip, shear-lag and time-dependent effects; (2) a dynamic analysis model considering the slip and shear lag effects of composite bridge–train coupling systems. The two models have been proposed by Zhu et al. [33–35]. The correctness and applicability of the two models have been verified by comparison with the corresponding experimental results [33–35]. Indeed, the long-term displacement of composite beams generated by the time-dependent analysis model is superposed on track irregularities at the corresponding position, which is used in the dynamic analysis model to investigate the dynamic characteristics of the composite box-girder bridge–train coupling system considering time-dependent behavior. The time-dependent behavior of composite box-girder bridges amplifies the dynamic characteristics of the composite girder bridge–train coupling system.

Selecting one carriage of a CRH2 high-speed train (the simplified model and essential parameters of the train are illustrated in Figure 1 and Table 1, respectively) passing through a simply supported 3 × 40 m steel-concrete composite box-girder bridge of a single-track railway as an example, the contributing factors of the time-dependent effect on the dynamic response of the composite box-girder bridge–train coupling system is investigated. The authors of [33] give the notation shown in Figure 1 and Table 1. This notation reflects the mechanical and geometric parameters of train. Figure 2 and Table 2 give the geometric parameters and the corresponding values of the composite bridge. In Table 2, ρ_{sh} is the shear stiffness of the interface of composite box-girder bridges. Table 3 gives the material parameters and the corresponding values of the composite bridge. In Table 3, f_{ck} is the cubic compressive strength of concrete at the 28th day, RH is the ambient relative humidity, t_{sh} is the curing age of concrete, ρ_c is the density of reinforced concrete, ρ_s is the density of steel, p_z is the dead load of ancillary facilities of the bridge deck, E_{s} is the elastic modulus of steel, and v_{c} and v_{s} are the Poisson's ratio of concrete and steel, respectively. The constitutive relationships based on time of the shrinkage strain and creep function referring to the CEB-FIP 90 [36] are utilized for the time-dependent analytical model of the composite box-girder bridges. The German high-speed spectrum [37] for track irregularity is selected for the dynamic analytical model of the composite box-girder bridge–train coupling system.

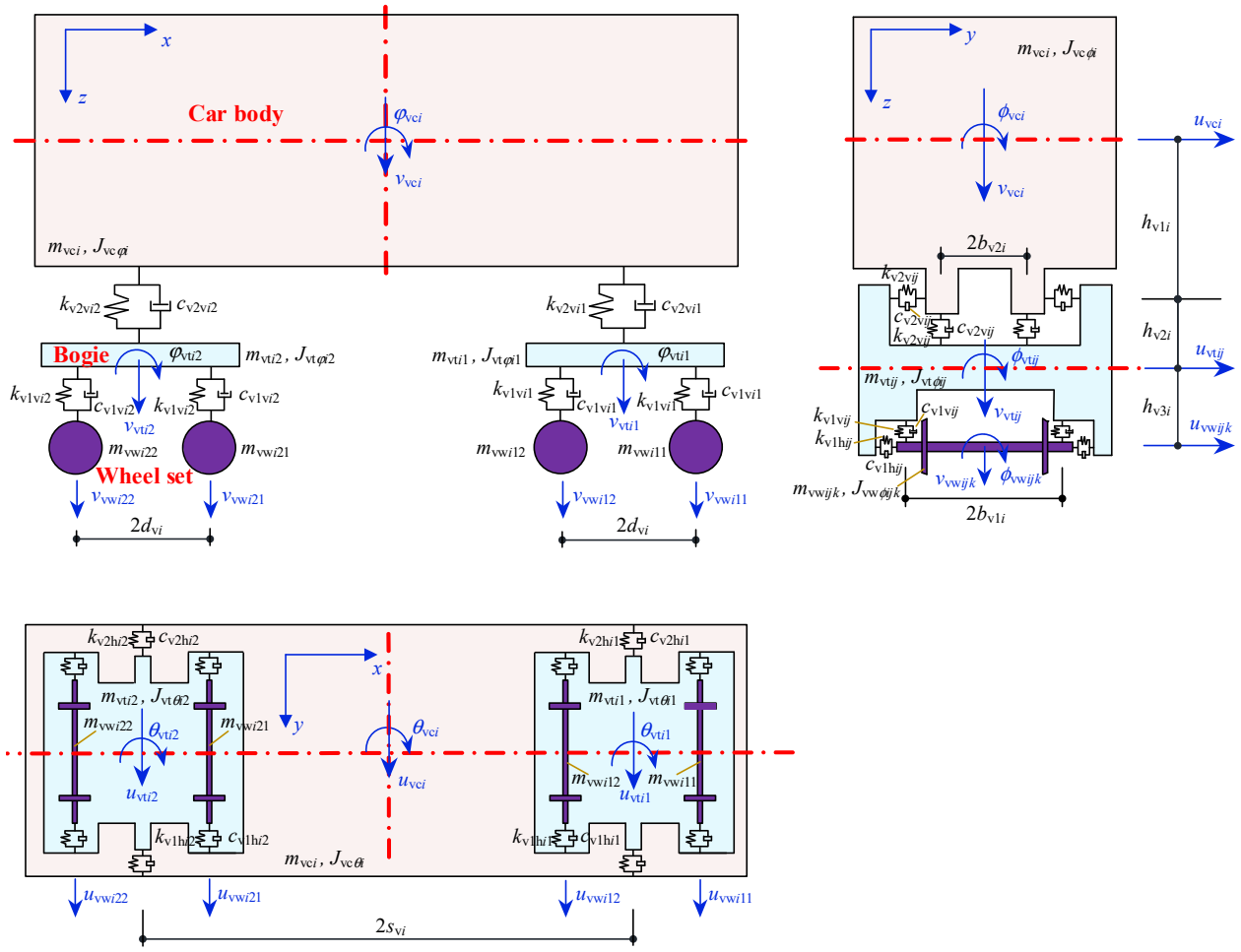

Figure 1. 27 DOF train model [33].

Table 1. Dynamic parameters of the CRH2 train.

Item	Unit	Motor Car	Trailer
m_{vc}	t	39.6	34.4
$J_{vc\theta}$	t·m^2	128.304	111.456
$J_{vc\phi}$	t·m^2	1940.4	1453.4
$J_{vc\psi}$	t·m^2	1673.1	1685.6
m_{vt}	t	3.2	2.6
$J_{vt\theta}$	t·m^2	2.592	2.106
$J_{vt\phi}$	t·m^2	3.2	2.6
$J_{vt\psi}$	t·m^2	1.752	1.423
m_{vw}	t	2	2.1
$J_{vw\theta}$	t·m^2	0.72	0.756
k_{v1h}	kN/m	7000	7000
k_{v1v}	kN/m	1000	1000
k_{v2h}	kN/m	360	360
k_{v2v}	kN/m	400	400
c_{v1h}	kN·s/m	0	0
c_{v1v}	kN·s/m	40	40
c_{v2h}	kN·s/m	100	100
c_{v2v}	kN·s/m	200	200
d_v	m	2.5	2.5
b_{v1}	m	2	2
b_{v2}	m	2	2
s_v	m	17.5	17.5
h_{v1}	m	1.7	1.7
h_{v2}	m	0.14	0.14
h_{v3}	m	0.28	0.28
h_{v4}	m	1.645	1.645

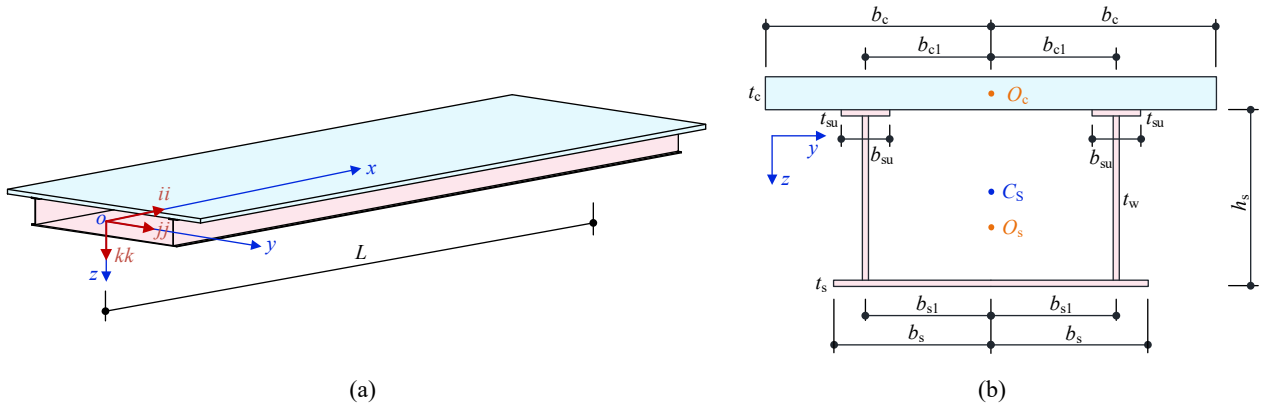

(a) (b)

Figure 2. Diagrams of steel-concrete composite box-girder bridges [33] (**a**) Three-dimension; (**b**) Cross-section.

Table 2. Geometric section of steel-concrete composite box-girder bridges.

b_c/mm	b_{c1}/mm	t_c/mm	b_s/mm	b_{s1}/mm	t_s/mm	b_{su}/mm	t_{su}/mm	h_s/mm	t_w/mm	ρ_{sh}/kN·mm^{-2}
5000	3000	300	3400	3000	40	500	30	3500	30	10

ρ_{sh} = 10 kN/mm^2 is a parameter applied in the design of practical composite girder bridges.

Table 3. Material properties and load parameters of the simply supported composite box-girder bridge.

f_{ck}/MPa	v_c	E_s/MPa	v_s	RH	t_{sh}/day	ρ_c/kg·m^{-3}	ρ_s/kg·m^{-3}	p_z/kN·m^{-1}
50	0.2	2.06×10^5	0.3	0.85	7	2500	7850	140

Figure 3 gives the change in vertical displacement of the composite box-girder bridge with time when the composite bridge is subjected to a dead load of self-weight and ancillary facilities. Figure 3a reflects the change in displacement distribution along the span at four time points, and Figure 3b shows the change in vertical displacement at mid-span with time. It can be observed that the vertical displacement increases with time, and the change rate diminishes with time. The increasing vertical displacement will become the new excitation of the train-bridge coupling system and amplify the dynamic responses of the system. However, there is no smooth transition of the vertical displacement at the supports between the two simply supported bridges, as shown in Figure 3a. This is not consistent with the actual case because of the existence of the track. Thus, the vertical displacement distribution curves along the span need to be fitted to be a set of smooth curves. Figure 4 shows the comparison between the calculated and the fitted displacement distribution curves at the 10th year. The fitting formula is given in Equation (1). The specific value of each coefficient in the fitting Equation (1) is given in Table 4.

$$y = \sum_{i=1}^{7} a_i \sin(b_i x + c_i) \quad (1)$$

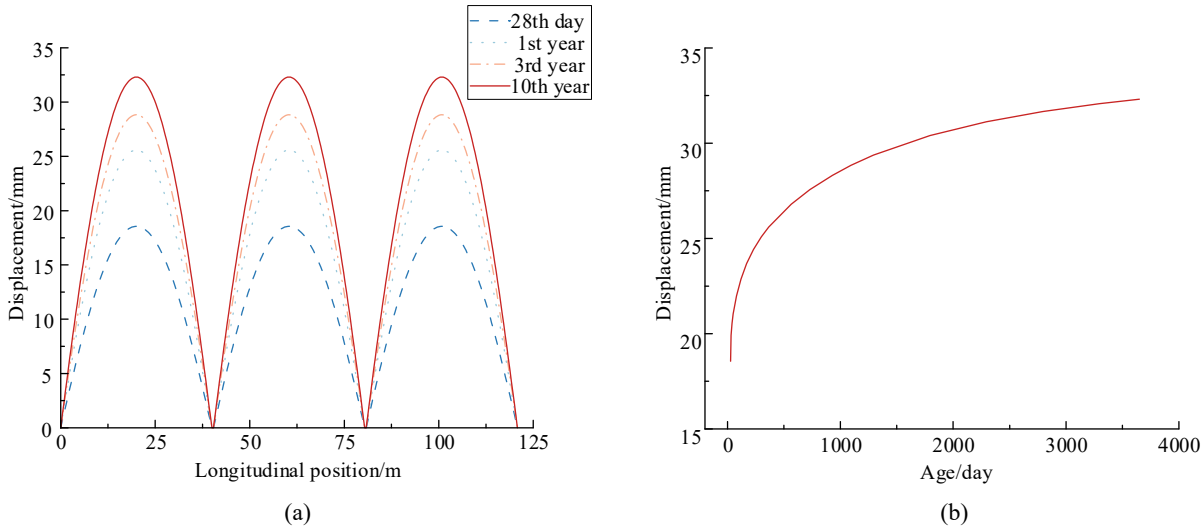

Figure 3. Change in vertical displacement of the composite box-girder bridge with time (**a**) Longitudinal distribution; (**b**) Change with time.

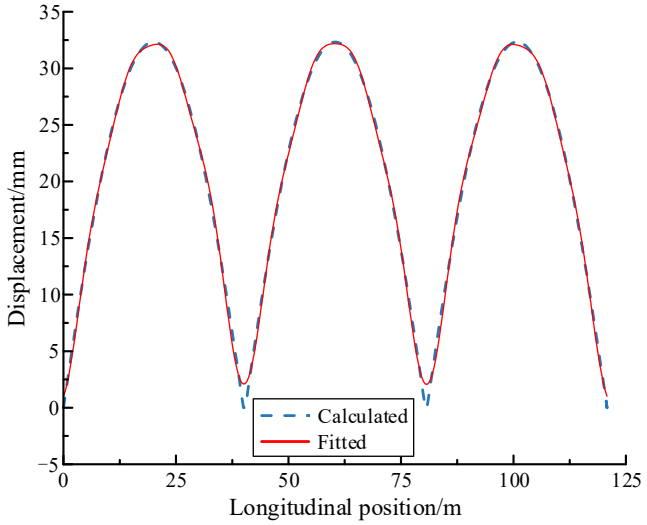

Figure 4. Comparison between the calculated and the fitted displacement distribution curves.

Table 4. Specific value of each coefficient in the fitting Equation (1).

i	a_i	b_i	c_i
1	36.38	0.02842	−0.1458
2	13.02	0.1573	−1.646
3	22.92	0.05556	1.356
4	7.978	0.08141	2.937
5	2.932	0.3101	−1.454
6	1.266	0.4631	−1.265
7	0.6798	0.6136	−0.9305

2.2. Influence on the Dynamic Responses of the Steel-Concrete Composite Bridge

This paper selects the vertical displacement and vertical acceleration in the mid-span of a bridge as the research objects to explore the influence of the time-dependent effect on the dynamic response of steel-concrete composite bridges under the self-excitation of CRH2 high-speed trains. The mid-span vertical displacement and the vertical acceleration both in time-history and frequency domain, including when transient, or at the 28th day,

3rd year and 10th year, are obtained when a train passes through the composite box-girder bridge at a speed of 300 km/h, as shown in Figures 5 and 6, respectively. At different operation times, the characteristic frequency relative to the mid-span vertical dynamic displacement of the composite box-girder bridge is 0.31 Hz. The change in operation time does not change the characteristic frequency distribution relative to the vertical displacement of the steel-concrete composite box-girder bridge. However, the dynamic response of vertical displacement increases with time. At different operation times, the characteristic frequency of vertical acceleration at the mid-span of the composite box-girder bridge slightly fluctuates, as shown in Table 5. Therefore, the change in time will slightly affect the characteristic frequency distribution relative to the vertical acceleration of the composite box-girder bridge. The dynamic response of vertical acceleration increases with time.

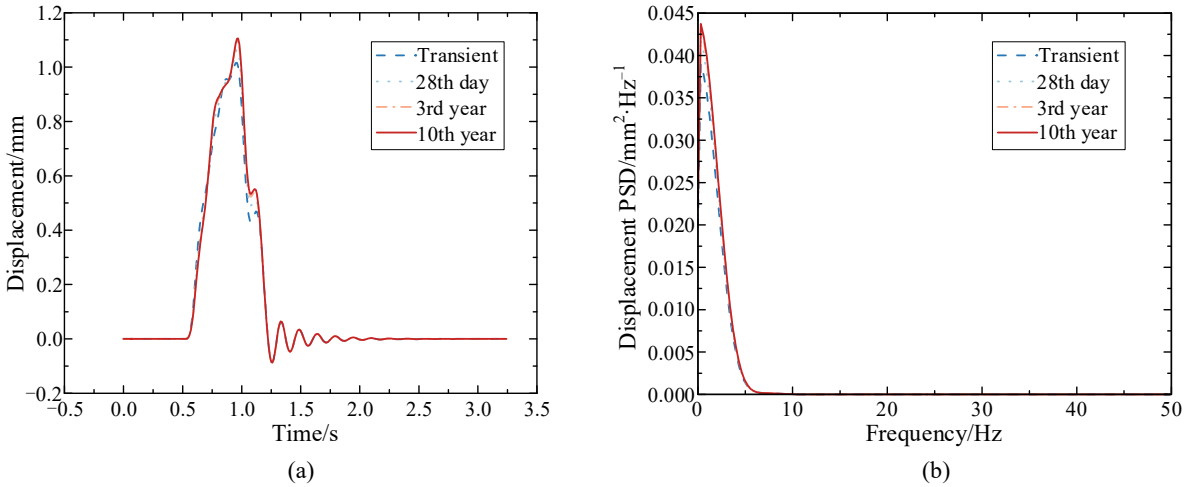

Figure 5. Vertical displacement of the mid-span section of the composite box-girder bridge at different operation times (**a**) Time history; (**b**) Power spectral density.

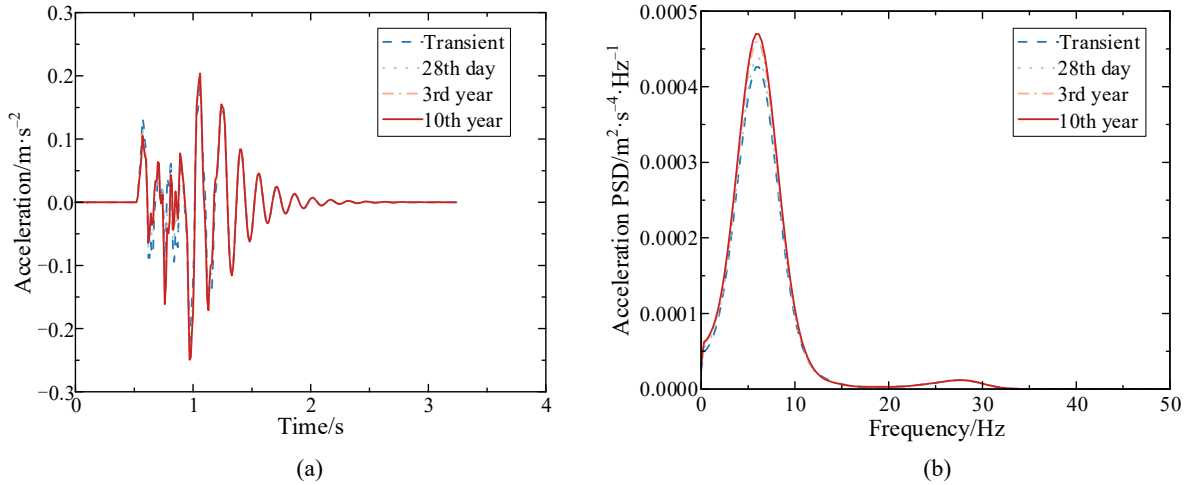

Figure 6. Vertical acceleration of the mid-span section of the composite box-girder bridge at different operation times (**a**) Time history; (**b**) Power spectral density.

Figures 7 and 8 exhibit the maximum of vertical displacement and vertical acceleration, respectively, at the mid-span of the composite box-girder bridge at different operation times within the time range as a whole when high-speed trains pass through it. The maximum vertical displacement at the mid-span of the composite bridge increases with time, from 1.02 mm in the transient case to 1.11 mm in the 10th year. The increase in the maximum of its vertical displacement slows with time. The maximum value of vertical acceleration at

the mid-span of the composite bridge increases with operation time, from 0.22 m/s^2 in the transient case to 0.25 m/s^2 in the 10th year. The increase in vertical acceleration slows with time. The time-dependent effect increases the maximum value of vertical displacement and vertical acceleration at the mid-span of the composite box-girder bridge by 8.82% and 13.64%, respectively. Compared with the vertical displacement, the time-dependent effect imposes a greater influence on the vertical acceleration of the composite bridge.

Table 5. Characteristic frequency relative to the vertical acceleration at the mid-span vertical acceleration of the second span for different operation stages.

Operation Stage	Transient	28th Day	3rd Year	10th Year
1st characteristic frequency/Hz	6.15	5.85	5.85	5.85
2nd characteristic frequency/Hz	27.69	27.69	27.69	27.69

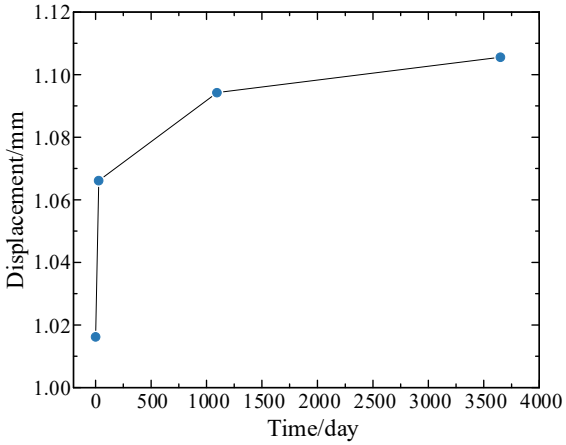

Figure 7. Maximum vertical displacements at the mid-span section of the composite box-girder bridge at various operation times.

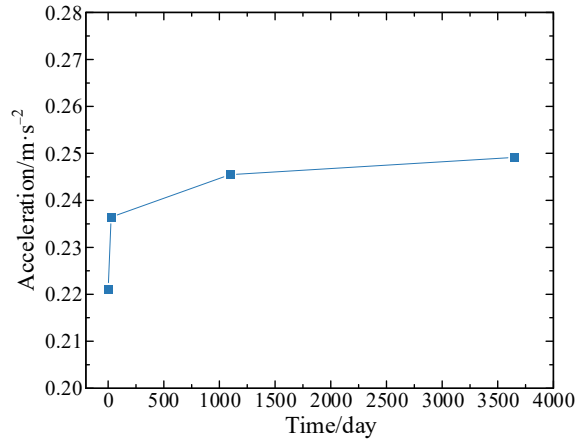

Figure 8. Maximum vertical accelerations at the mid-span section of the composite box-girder bridge at various operation times.

2.3. Influence on the Dynamic Responses of the Train

The composite box-girder bridge–train coupling system is a coupling system. The analysis in Section 2.1 has revealed that the time-dependent effect has a significant impact on the dynamic responses of the composite box-girder bridge. It can be predicted that the time-dependent effect is bound to impose a significant influence on the dynamic responses of the train. In this paper, the vertical acceleration of the train body is selected. When one carriage of the CRH2 high-speed train passes through the composite box-girder bridge

with transient operation times including the 28th day, 3rd year and 10th year at a speed of 300 km/h, the vertical acceleration of the train body in the time history and frequency domain are summarized in Figure 9, and the maximum values of the vertical acceleration of the train body at different operation times are summarized in Figure 10. The characteristic frequency of train vertical acceleration is slightly different under different operation time conditions. The frequency is 4.62 Hz in the transient case, 1.54 Hz on the 28th day, and 0.31 Hz at the 3rd and 10th years. The change in time will have an impact on the distribution of the train's characteristic frequency. The dynamic response increases more significantly with time compared with the characteristic frequency. As illustrated in Figure 10, the maximum vertical acceleration of the train body increases with operation time, going from 0.67 m/s^2 in the instantaneous case to 1.64 m/s^2 in the 10th year. The increase in amplitude slows with increasing operation time. The time-dependent effect will increase the maximum vertical acceleration of the train by 144.78% from the transient case to the 10th year.

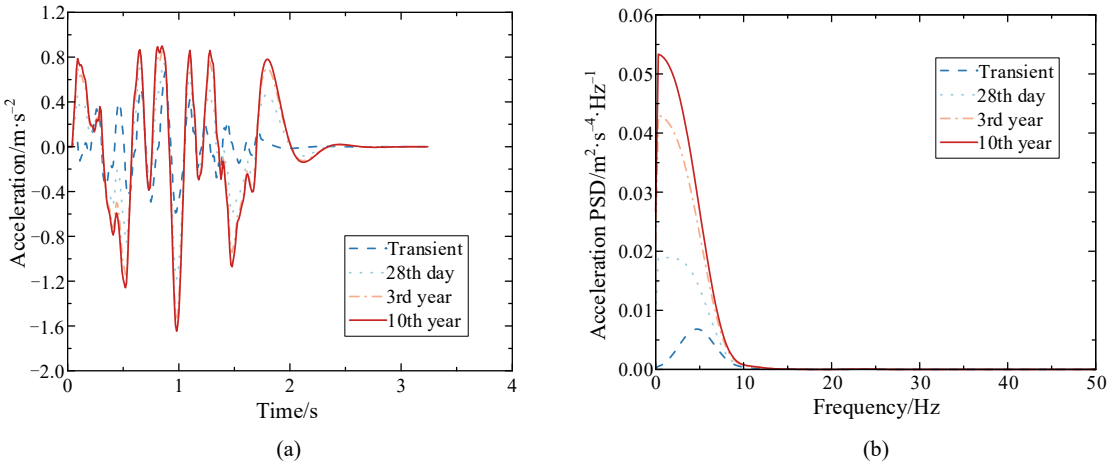

Figure 9. Vertical acceleration of the train at different operation times (**a**) Time history; (**b**) Power spectral density.

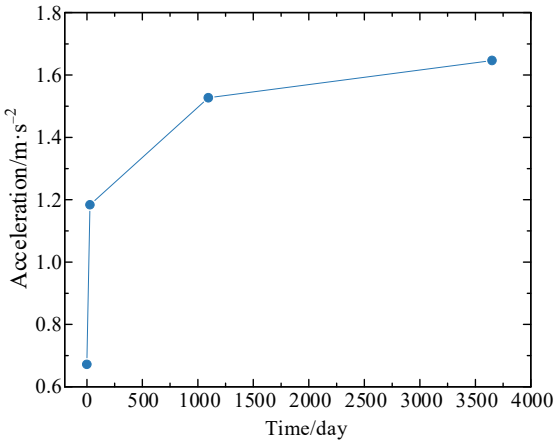

Figure 10. Maximum vertical accelerations of the train at various operation times.

3. Effect of the Slip Effect on the Dynamic Responses of a Composite Bridge–Train Coupling System with the Time-Dependent Behavior

Relevant studies have shown that the slip between the interface of the concrete slab and the steel box-girder of composite beams is basically caused by the shear deformation of shear connectors. Thus, this paper simulates the shear deformation characteristics of shear connectors by setting different shear connection stiffnesses. The effect law of the slip effect of the CRH2 high-speed train on the dynamic responses of the composite box-girder bridge–train coupling system with a time-dependent behavior is obtained.

3.1. Effect of the Slip on the Dynamic Responses of Steel-Concrete Composite Bridges

The case keeps the same as above. The responses of the vertical displacement and vertical acceleration of the composite box-girder bridge with shear connection stiffness ρ_{sh} = 1 kN/mm^2 in the transient case, 28th day, 3rd year and 10th year are illustrated in Figures 11 and 12, respectively. The dynamic responses such as the vertical displacement and acceleration of the composite box-girder bridge with shear connection stiffness ρ_{sh} = 100 kN/mm^2 at the transient time, 28th day, 3rd year and 10th year are illustrated in Figures 13 and 14, respectively. The maximum vertical displacement and vertical acceleration curves at different operation times are illustrated in Figures 15 and 16, respectively.

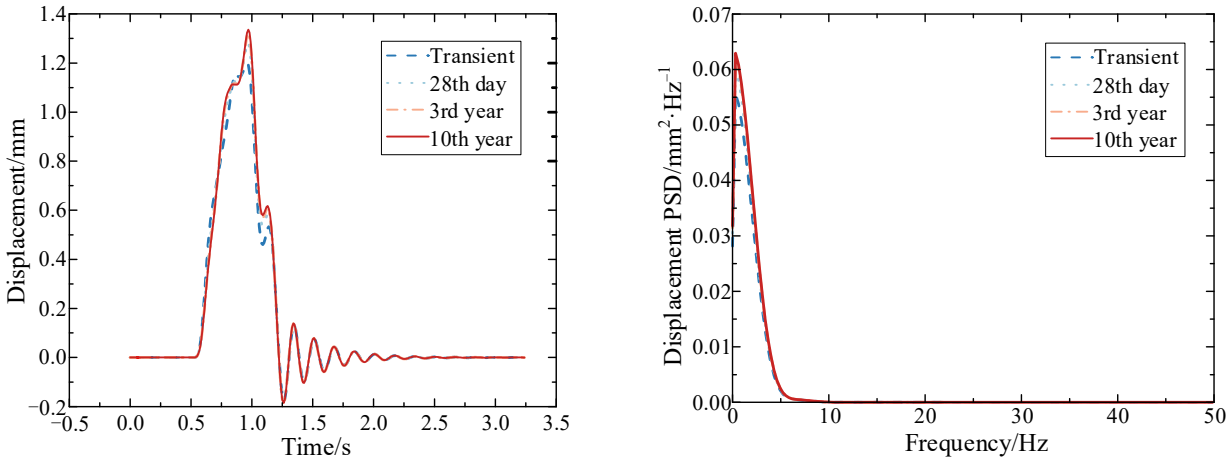

Figure 11. Vertical displacement of the mid-span section of the composite girder bridge when ρ_{sh} = 1 kN/mm^2 (**a**) Time history; (**b**) Power spectral density.

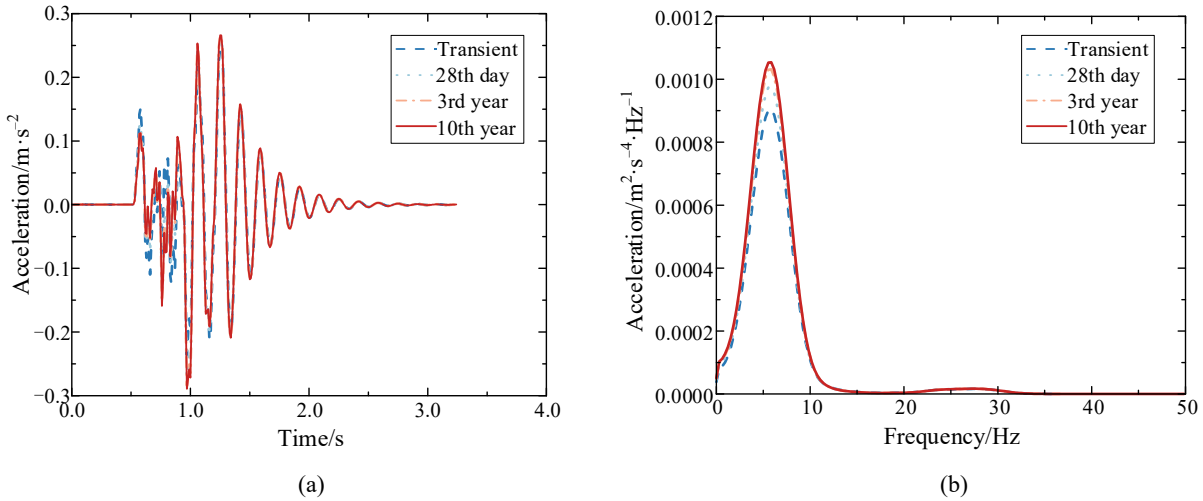

Figure 12. Vertical acceleration at the mid-span section of the composite girder bridge when ρ_{sh} = 1 kN/mm^2 (**a**) Time history; (**b**) Power spectral density.

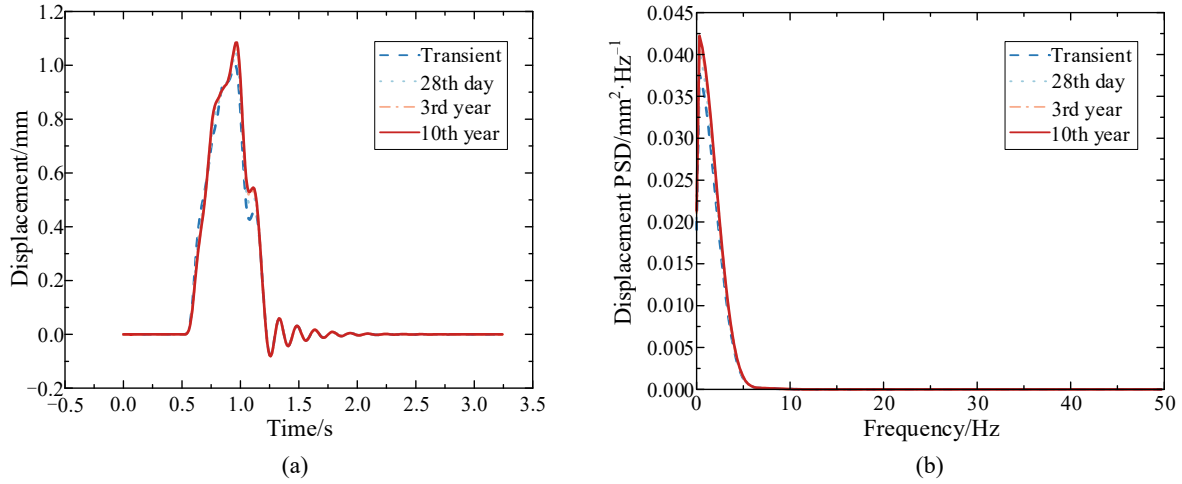

Figure 13. Vertical displacement at the mid-span section of the composite girder bridge when ρ_{sh} = 100 kN/mm^2 (**a**) Time history; (**b**) Power spectral density.

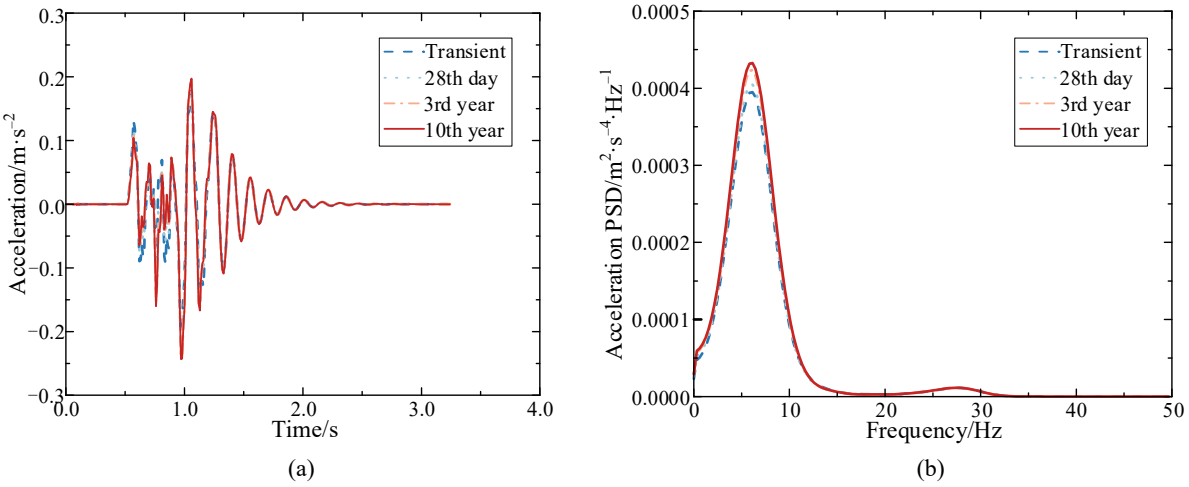

Figure 14. Vertical acceleration at the mid-span section of the composite girder bridge when ρ_{sh} = 100 kN/mm^2 (**a**) Time history; (**b**) Power spectral density.

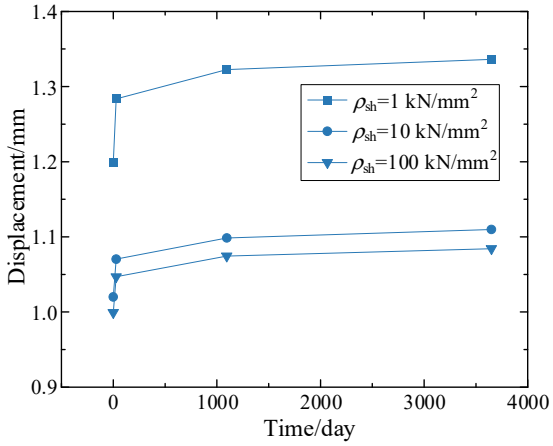

Figure 15. The maximum vertical displacements at the mid-span section of the composite girder bridge with various operation times.

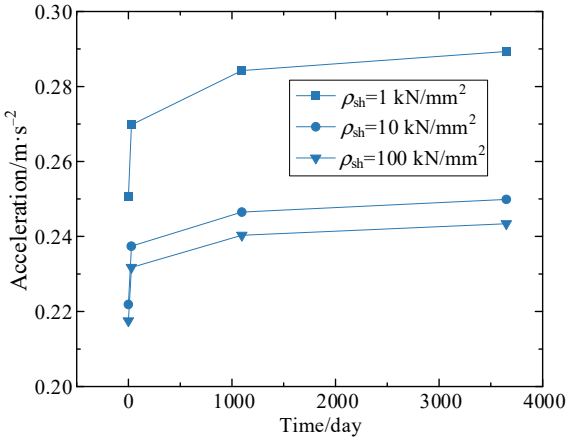

Figure 16. The maximum vertical accelerations at the mid-span section of the composite girder bridge with various operation times.

From the results, the increase in shear connection stiffness reduces the vertical displacement amplitude of the steel–concrete composite beam at different operation times but will not affect the trend that the growth rate slows with increasing operation time. When the shear connection stiffnesses of the composite box-girder bridge are ρ_{sh} = 1 kN/mm^2, ρ_{sh} = 10 kN/mm^2 and ρ_{sh} = 100 kN/mm^2, the mid-span vertical displacements in the 10th year are 1.34 mm, 1.11 mm and 1.08 mm, respectively; At the transient time, the mid-span vertical displacements are 1.20 mm, 1.02 mm and 1.00 mm. The data in the frequency domain in Figures 5, 11 and 13 reveal that the slip does not influence the distribution of the vertical displacement characteristic frequency under the time-dependent behavior of the steel-concrete composite box-girder bridge. When the shear connection stiffnesses are ρ_{sh} = 1 kN/mm^2, ρ_{sh} = 10 kN/mm^2 and ρ_{sh} = 100 kN/mm^2, the characteristic frequencies relative to the vertical displacement are equivalent at different operation times, that is, the slip does not change the characteristic frequency relative to the vertical displacement at the mid-span of the composite box-girder bridge. However, it is notable that the slip does affect the maximum value of dynamic responses.

The effect law of the slip on the vertical acceleration is, to some degree, similar to that on the vertical displacement. The greater the shear connection stiffness is, the lower the dynamic response. The slip effect does not affect the trend that the growth rate slows with operation time. When the shear connection stiffnesses of the composite bridge are ρ_{sh} = 1 kN/mm^2, ρ_{sh} = 10 kN/mm^2 and ρ_{sh} = 100 kN/mm^2, the mid-span vertical accelerations in the 10th year are 0.29 m/s^2, 0.25 m/s^2 and 0.24 m/s^2, respectively; for the transient case, the mid-span vertical accelerations are 0.25 m/s^2, 0.22 m/s^2, and 0.217 m/s^2. When the shear connection stiffnesses are ρ_{sh} = 1 kN/mm^2, ρ_{sh} = 10 kN/mm^2 and ρ_{sh} = 100 kN/mm^2, the characteristic frequencies relative to vertical acceleration are shown in Table 6. Therefore, the slip has little influence on the distribution of the characteristic frequency relative to vertical acceleration under the time-dependent behavior. However, note that the existence of slip affects the dynamic response value, which decreases with increasing shear connection stiffness.

Table 6. Characteristic frequencies at the mid-span vertical acceleration of the second span with different shear connection stiffnesses.

Operation Stage		Transient	28th Day	3rd Year	10th Year
ρ_{sh} = 1 kN/mm^2	Characteristic frequency/Hz	5.85	5.85	5.85	5.85
	Characteristic frequency/Hz	27.38	27.38	27.38	27.38
ρ_{sh} = 10 kN/mm^2	Characteristic frequency/Hz	6.15	5.85	5.85	5.85
	Characteristic frequency/Hz	27.69	27.69	27.69	27.69
ρ_{sh} = 100 kN/mm^2	Characteristic frequency/Hz	6.15	6.15	6.15	6.15
	Characteristic frequency/Hz	27.69	27.69	27.69	27.69

3.2. Effect of Slip on Dynamic Responses of the Train

The dynamic responses of the vertical acceleration of the train body for composite bridges with shear connection stiffness ρ_{sh} = 1 kN/mm^2, in the transient case and at the 28th day, 3rd year and 10th year are illustrated in Figure 17. The dynamic responses of the vertical acceleration of the train body for composite box-girder bridges with shear connection stiffness ρ_{sh} = 100 kN/mm^2, in the transient case and at the 28th day, 3rd year and 10th year are shown in Figure 18. The maximum vertical acceleration curves of the train body at different operation times are illustrated in Figure 19.

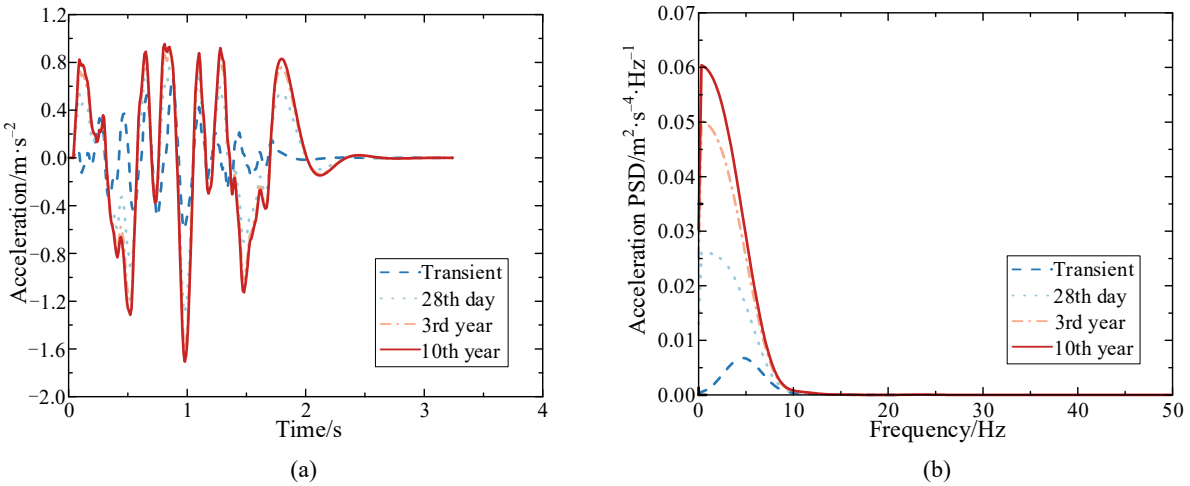

(a) (b)

Figure 17. Vertical acceleration of the train body when ρ_{sh} = 1 kN/mm^2 (**a**) Time history; (**b**) Power spectral density.

From the vertical acceleration results, the increase in the train-body shear connection stiffness slightly reduces the dynamic response amplitude but will not affect the trend that the growth rate slows with increasing operation time. When the shear connection stiffnesses of the composite box-girder bridge are ρ_{sh} = 1 kN/mm^2, ρ_{sh} = 10 kN/mm^2, and ρ_{sh} = 100 kN/mm^2, the vertical accelerations of the train body in the 10th year are 1.71 m/s^2, 1.65 m/s^2, and 1.64 m/s^2, respectively; for the instantaneous case, the vertical accelerations of the train body are 0.68 m/s^2, 0.67 m/s^2, and 0.67 m/s^2, respectively. The results in the frequency domain in Figures 9, 17 and 18 reveal that when the shear connection stiffnesses are ρ_{sh} = 1 kN/mm^2, ρ_{sh} = 10 kN/mm^2 and ρ_{sh} = 100 kN/mm^2, respectively, the characteristic frequencies relative to the vertical acceleration do not change (refer to Table 7). The existence of slip does not change the distribution of the characteristic frequencies relative to the train vertical accelerations under the time-dependent effect. However, note that the existence of slip affects the dynamic response value, which decreases with increasing interface connection stiffness.

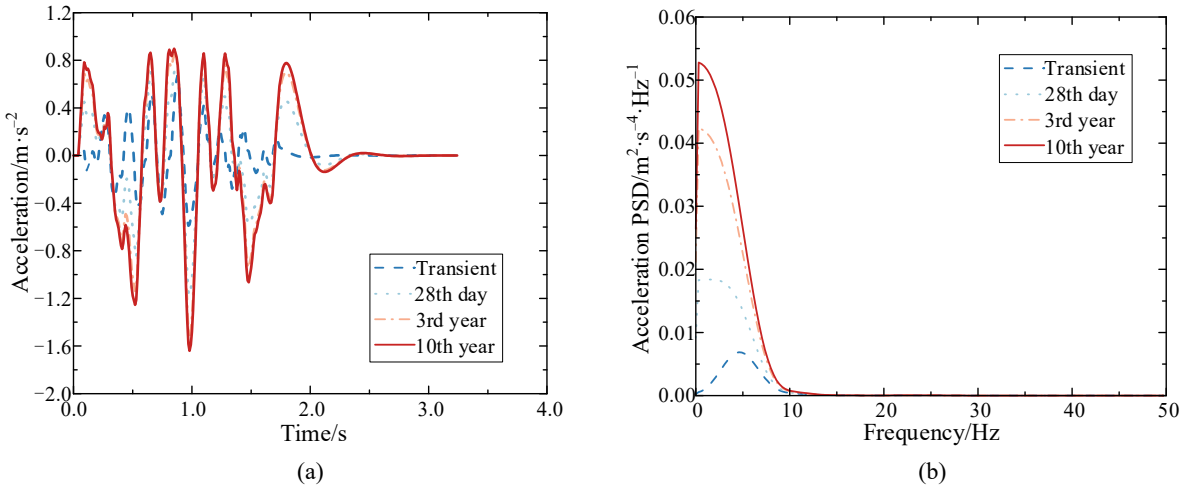

Figure 18. Vertical acceleration of the train body when ρ_{sh} = 100 kN/mm^2 (**a**) Time history; (**b**) Power spectral density.

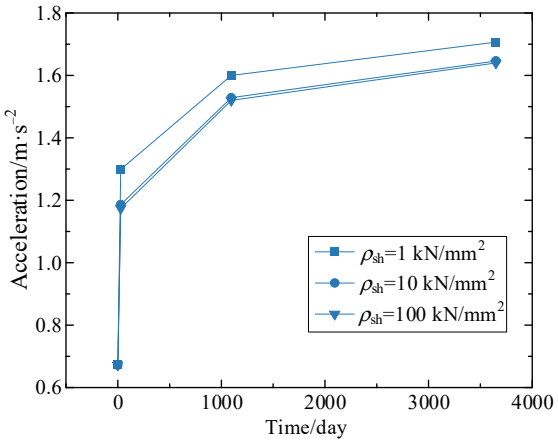

Figure 19. Maximum vertical accelerations of the train body for various shear connection stiffnesses.

Table 7. Characteristic frequencies of train body vertical acceleration for different shear connection stiffnesses.

Operation Stage		Transient	28th Day	3rd Year	10th Year
ρ_{sh} = 1 kN/mm^2	Characteristic frequency/Hz	4.61	0.31	0.31	0.31
ρ_{sh} = 10 kN/mm^2	Characteristic frequency/Hz	4.61	1.54	0.31	0.31
ρ_{sh} = 100 kN/mm^2	Characteristic frequency/Hz	4.61	1.54	0.31	0.31

4. Effect of the Shear Lag on the Dynamic Responses of a Composite Girder Bridge–Train Coupling System under Time-Dependent Behavior

Relevant studies show that the shear lag effect should be taken into consideration when the flange of a beam is wide. In this paper, two cases with and without considering the shear lag of steel-concrete composite box-girder bridges are compared. The influence law of the shear lag on the dynamic responses of the composite girder bridge–train coupling system under time-dependent behavior is obtained and analyzed.

4.1. Effect of the Shear Lag on the Dynamic Responses of Steel-Concrete Composite Girder Bridges

The case remains the same as above. The dynamic responses of the vertical displacement and vertical acceleration of the composite box-girder bridge without the consideration of the shear lag effect at a transient time and at the 28th day, 3rd year and 10th year are

illustrated in Figures 20 and 21, respectively. The maximum vertical displacement and vertical acceleration curves at different operation times are shown in Figures 22 and 23, respectively.

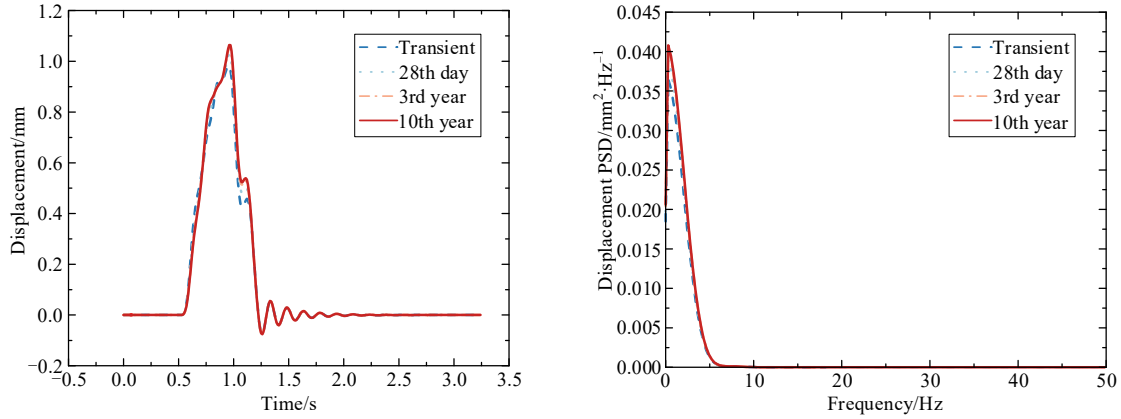

Figure 20. Vertical displacement at the mid-span section of the composite bridge without considering the shear lag effect (**a**) Time history; (**b**) Power spectral density.

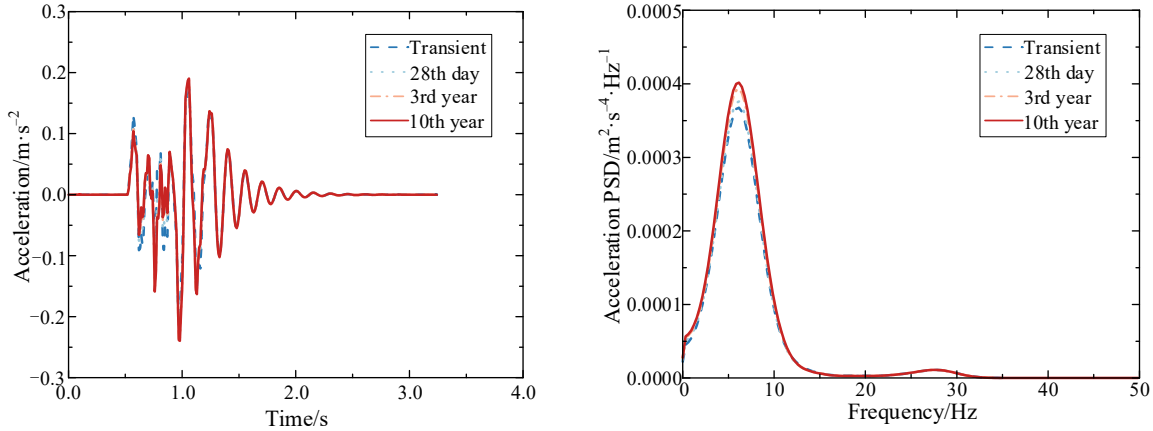

Figure 21. Vertical acceleration at the mid-span section of the composite bridge without considering the shear lag effect (**a**) Time history; (**b**) Power spectral density.

Figures 20 and 21 reveal the change in vertical displacement and acceleration with time at the mid-span of the composite box-girder bridge without considering the shear lag effect. The characteristic frequency relative to the mid-span vertical displacement of the composite box-girder bridge without the shear lag effect is 0.31 Hz at different operation times, and the change in operation time does not change the characteristic frequency distribution relative to the vertical displacement. The dynamic response of the vertical displacement slightly increases with time. The characteristic frequency relative to the vertical acceleration of the composite bridge without the shear lag is slightly different from that considering the shear lag effect, as shown in Table 8. A comparison of Figures 6 and 21 shows that the shear lag affects the distribution of characteristic frequencies relative to the vertical acceleration of the composite box-girder bridge. The shear lag increases the dynamic responses of the vertical displacement and vertical acceleration of the composite box-girder bridge but does not affect the change trend of their time-history curves.

Figures 22 and 23 show the maximum vertical displacements and maximum vertical accelerations, respectively, at the mid-span of the composite box-girder bridge at different operation times within the whole time range of train passage. The maximum

vertical displacements and vertical accelerations at mid-span increase with the operation time going.

Table 8. Characteristic frequencies of the mid-span vertical acceleration of the second span with and without considering the shear lag effect.

Operation Stage		Transient	28th Day	3rd Year	10th Year
With shear lag	1st characteristic frequency/Hz	6.15	6.15	5.85	5.85
	2nd characteristic frequency/Hz	27.69	27.69	27.69	27.69
Without shear lag	1st characteristic frequency/Hz	6.15	6.15	6.15	6.15
	2nd characteristic frequency/Hz	27.69	27.69	27.69	27.69

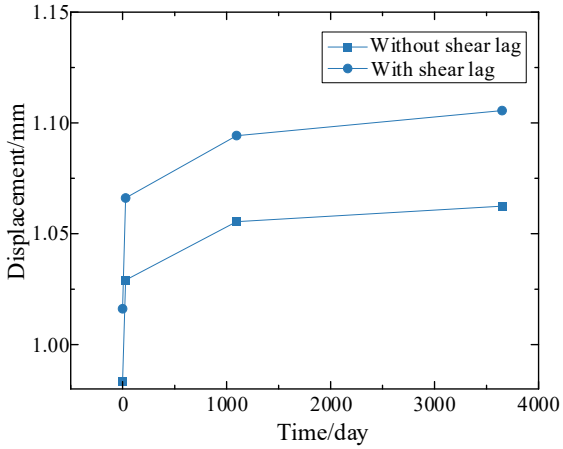

Figure 22. Maximum vertical displacements of the composite bridge without considering the shear lag effect with operation times.

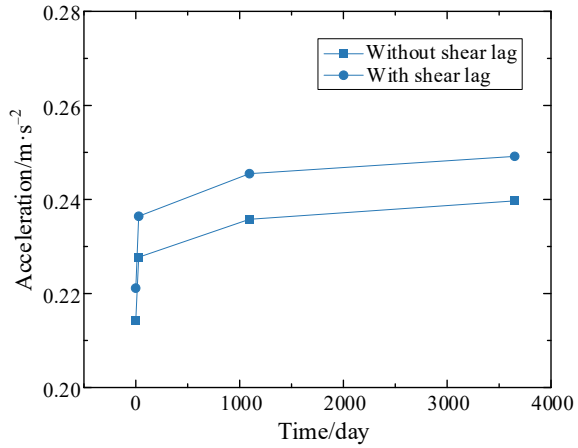

Figure 23. Maximum vertical accelerations of the composite bridge without considering the shear lag effect with operation times.

4.2. Effect of the Shear Lag on the Train Dynamic Responses

The responses of the vertical acceleration of the train body without the shear lag effect in the transient case and at the 28th day, 3rd year and 10th year are shown in Figure 24. The maximum vertical acceleration curves at different operation times are illustrated in Figure 25.

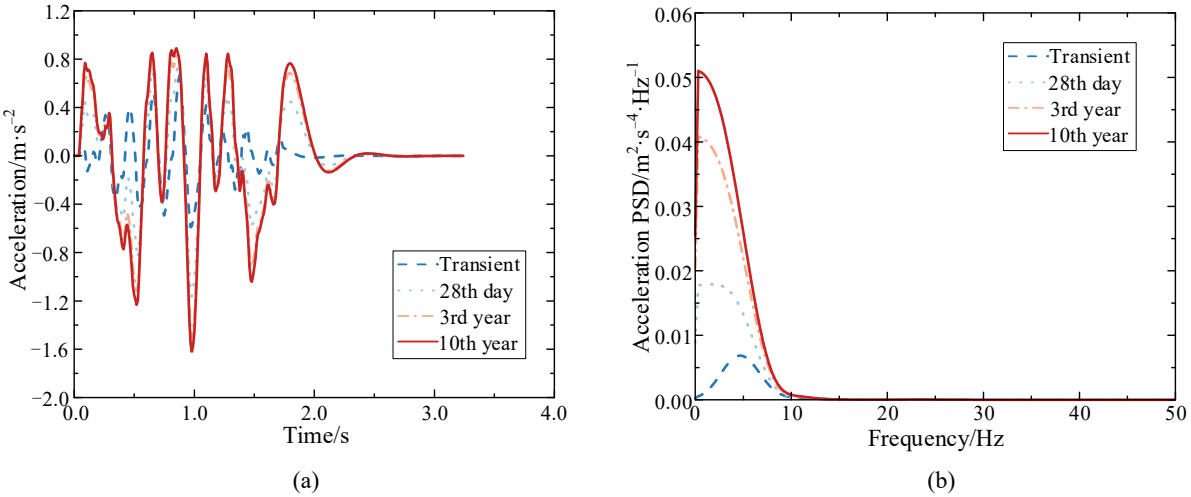

Figure 24. Vertical acceleration of the train body without considering the shear lag (**a**) Time history; (**b**) Power spectral density.

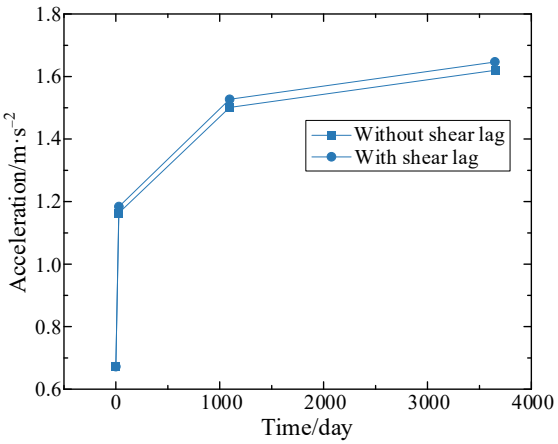

Figure 25. Maximum vertical accelerations of the train body with and without considering the shear lag with operation time.

Figure 24 reveals that the vertical acceleration of the train body increases with the operation time. The characteristic frequencies of vertical acceleration are different at different operation times. The characteristic frequency for the transient case is 4.62 Hz; for the 28th day 1.54 Hz; for the 3rd year 0.31 Hz and for the 10th year 0.31 Hz. The change in time slightly impacts the distribution characteristic frequency of the train body. The dynamic responses of the vertical acceleration of the train body also increase with time. Figure 25 shows that the maximum vertical acceleration of the train body increases with the operation time and that the rate of increase in amplitude slows with time.

The maximum vertical acceleration changes from 0.67 m/s^2 in the transient state to 1.62 m/s^2 in the 10th year. It can be seen that the existence of a time-dependent behavior increases the maximum vertical acceleration of the train body by 141.79%. A comparison of Figures 9 and 10 indicates that the shear-lag effect does not affect the rate of increase in the vertical acceleration of the train body with operation time and the trend of the time history curve nor does it affect the distribution of the characteristic frequencies of vertical acceleration of the train body under the time-dependent effect. However, the shear-lag effect reduces the maximum of vertical acceleration of the train body.

5. Conclusions

For the steel-concrete composite box-girder bridge, on the basis of the proposed time-dependent model and the proposed dynamic model of the train-bridge coupling system,

this paper established a computation program for the dynamic characteristics of composite box-girder bridge–train coupling systems with the time-dependent behavior at different operation times. The effect of the time-dependent behavior on the dynamic responses of the composite box-girder bridge–train coupling system was investigated. The conclusions that can be drawn are as follows:

(1) The maximum values of the vertical displacement and vertical acceleration at the mid-span of the steel-concrete composite box-girder bridge increased with the operation time. The maximum vertical displacement and acceleration increased by 8.82% and 13.64%, respectively, because of the time-dependent behavior. The time-dependent effect increased the maximum value of train-body vertical acceleration by 144.78%. Compared with the vertical displacement of the composite box-girder bridge, the time-dependent behavior had a greater impact on the vertical acceleration of both the bridge and train.

(2) The maximum of the vertical displacement and acceleration at the mid-span of the composite box-girder bridge and the maximum of the vertical acceleration of the train decreased with shear connection stiffness increasing at different operation times. However, the slip effect did not influence the change trend of the time-history curves. The vertical displacement of the composite box-girder bridge and the characteristic frequency distribution relative to the train vertical acceleration do not significantly change with a change in the shear connection stiffness under the time-dependent effect. The change in shear connection stiffness also has minimal impact on the characteristic frequency distribution of the vertical acceleration of the composite box-girder bridge. However, the dynamic responses increase more slowly with an increase in shear connection stiffness.

(3) For the vertical displacement and acceleration of the composite box-girder bridge and the vertical acceleration of the train body under the time-dependent effect, the shear-lag effect increased their responses but did not affect their growth trend with increasing operation time. The shear lag effect does not change the vertical displacement of the composite box-girder bridge or the characteristic frequency distribution of the vertical acceleration of the train body under the time-dependent effect. The effect has minimal impact on the characteristic frequency distribution of the vertical acceleration of the composite box-girder bridge. However, the dynamic response of the vertical acceleration of the bridge notably increases because of the shear lag effect.

Author Contributions: Conceptualization, L.Z.; methodology, L.Z.; validation, B.H.; formal analysis, C.G. and R.S.; investigation, C.G.; resources, L.Z.; data curation, B.H. and Q.-C.T.; writing—original draft preparation, R.S.; writing—review and editing, C.G.; visualization, C.G. and Q.-C.T.; supervision, L.Z.; project administration, L.Z. and C.G. All authors have read and agreed to the published version of the manuscript.

Funding: The research was funded by the Key R & D Projects of China State Railway Group Co., Ltd. (No. N2018G069) and the Key R & D Projects of China Railway Economic and Planning Research Institute Co., Ltd. (No. 2019YJJ02).

Institutional Review Board Statement: Not applicable.

Informed Consent Statement: Not applicable.

Data Availability Statement: The data provided in this study could be released upon reasonable request.

Conflicts of Interest: The authors declare no conflict of interest.

References

1. Chiorino, M.A.; Nopali, P.; Mola, F.; Koprna, M. CEB design manual on structural effects of time-dependent behaviour of concrete. *Weed Technol.* **1984**, *391*, 777–781.
2. Zdenek, P.; Baant, T.; Baweja, S. Creep and Shrinkage Prediction Model for Analysis and Design of Concrete Structures: Model B3. *Mater. Struct.* **1995**, *28*, 357–365.

3. Bazant, Z.P. Prediction of concrete creep effects using age-adjusted effective modulus method. *ACI J.* **1972**, *69*, 212–217.
4. Bazant, Z.P. Numerical determination of long-range stress history from strain history in concrete. *Mater. Struct.* **1972**, *5*, 135–141. [CrossRef]
5. Zhu, L.; Su, R. Analytical solutions for composite beams with slip, shear-lag and time-dependent effects. *Eng. Struct.* **2017**, *152*, 559–578. [CrossRef]
6. Gilbert, R.I.; Bradford, M.A. Time-Dependent Behavior of Continuous Composite Beams at Service Loads. *J. Struct. Eng.* **1995**, *121*, 319–327. [CrossRef]
7. Gattesco, N. Analytical modeling of nonlinear behavior of composite beams with deformable connection. *J. Constr. Steel Res.* **1999**, *52*, 195–218. [CrossRef]
8. Yan, J.B. Finite element analysis on steel-concrete–steel sandwich beams. *Mater. Struct.* **2014**, *48*, 1645–1667. [CrossRef]
9. Polanco, N.R.; May, G.; Hernandez, E.M. Finite element model updating of semi-composite bridge decks using operational acceleration measurements. *Eng. Struct.* **2016**, *126*, 264–277. [CrossRef]
10. Monetto, I.; Campi, F. Numerical analysis of two-layer beams with interlayer slip and step-wise linear interface law. *Eng. Struct.* **2017**, *144*, 201–209. [CrossRef]
11. Uddin, A.; Sheikh, A.H.; Brown, D.; Bennett, T.; Uy, B. A higher order model for inelastic response of composite beams with interfacial slip using a dissipation based arc-length method. *Eng. Struct.* **2017**, *139*, 120–134. [CrossRef]
12. Fabbrocino, G.; Manfredi, G.; Cosenza, E. Analysis of Continuous Composite Beams Including Partial Interaction and Bond. *J. Struct. Eng.* **2000**, *126*, 1288–1294. [CrossRef]
13. Oven, V.A.; Burgess, I.W.; Plank, R.J.; Abdul, A.A. An analytical model for the analysis of composite beams with partial shear interaction. *Comput. Struct.* **1997**, *62*, 493–504. [CrossRef]
14. Kolakowski, Z.; Kubiak, T. Some aspects of the longitudinal-transverse mode in the elastic thin-walled girder under bending moment. *Thin-Walled Struct.* **2016**, *102*, 197–204. [CrossRef]
15. Gara, F.; Ranzi, G.; Leoni, G. Short- and long-term analytical solutions for composite beams with partial interaction and shear-lag effects. *Int. J. Steel Struct.* **2010**, *10*, 359–372. [CrossRef]
16. Henriques, D.; Gonçalves, R.; Camotim, D. A physically non-linear GBT-based finite element for steel and steel-concrete beams including shear lag effects. *Thin-Walled Struct.* **2015**, *90*, 202–215. [CrossRef]
17. Henriques, D.; Gonçalves, R.; Camotim, D. GBT-based finite element to assess the buckling behaviour of steel–concrete composite beams. *Thin-Walled Struct.* **2016**, *107*, 207–220. [CrossRef]
18. Zhu, L.; Nie, J.G.; Li, F.X.; Ji, W.Y. Simplified analysis method accounting for shear-lag effect of steel–concrete composite decks. *J. Constr. Steel Res.* **2015**, *115*, 62–80. [CrossRef]
19. Zhang, Y.-H.; Lin, L.-X. Shear lag analysis of thin-walled box girders based on a new generalized displacement. *Eng. Struct.* **2014**, *61*, 73–83. [CrossRef]
20. Sapountzakis, E.; Tsiptsis, I. Generalized warping analysis of curved beams by BEM. *Eng. Struct.* **2015**, *100*, 535–549. [CrossRef]
21. Frýba, L. *Vibration of Solids and Structures under Moving Loads*; Thomas Telford: London, UK, 1999.
22. Timonshenko, S.P. CV. On the force vibration of bridges. *Lond. Edinb. Dublin Philos. Mag. J. Sci.* **1992**, *43*, 1018–1019. [CrossRef]
23. Muchnikov, Y.M. Some methods of computing vibration of elastic systems subjected to moving loads. *Gosstroiizdat Mosc.* **1953**, *19*, 216–223.
24. Wang, L.; Kang, X.; Jiang, P. Vibration analysis of a multi-span continuous bridge subject to complex traffic loading and vehicle dynamic interaction. *KSCE J. Civ. Eng.* **2015**, *20*, 323–332. [CrossRef]
25. Ju, S.-H. Vibration Analysis of 3D Timoshenko Beams Subjected to Moving Vehicles. *J. Eng. Mech.* **2011**, *137*, 713–721. [CrossRef]
26. Nassif, H.H.; Liu, M.; Ertekin, O. Model validation for bridge-road-vehicle dynamic interaction system. *J. Bridge Eng.* **2003**, *8*, 112–120. [CrossRef]
27. Law, S.; Zhu, X. Bridge dynamic responses due to road surface roughness and braking of vehicle. *J. Sound Vib.* **2005**, *282*, 805–830. [CrossRef]
28. Moghimi, H.; Ronagh, H.R. Development of a numerical model for bridge–vehicle interaction and human response to traffic-induced vibration. *Eng. Struct.* **2008**, *30*, 3808–3819. [CrossRef]
29. Zhou, W.-B.; Jiang, L.-Z.; Yu, Z.-W. Analysis of free vibration characteristic of steel-concrete composite box-girder considering shear lag and slip. *J. Central South Univ.* **2013**, *20*, 2570–2577. [CrossRef]
30. Wang, H.; Zhu, E. Dynamic response analysis of monorail steel-concrete composite beam-train interaction system considering slip effect. *Eng. Struct.* **2018**, *160*, 257–269. [CrossRef]
31. Uiker-Kaustell, M.; Karoumi, R. Application of the continuous wavelet transform on the free vibrations of a steel-concrete composite railway bridge. *Eng. Struct.* **2011**, *33*, 911–919. [CrossRef]
32. Liu, K.; Reynders, E.; Roeck, G.D.; Lombaert, G. Experimental and numerical analysis of a composite bridge for high-speed trains. *J. Sound Vib.* **2009**, *320*, 201–220.
33. Zhu, L.; Wang, H.-L.; Han, B.; Zhao, G.-Y.; Huo, X.-J.; Ren, X.-Z. Dynamic analysis of a coupled steel-concrete composite box girder bridge-train system considering slip and shear-lag. *Thin-Walled Struct.* **2020**, *157*, 107060. [CrossRef]
34. Zhu, L.; Zhao, G.-Y.; Su, R.K.-L.; Liu, W.; Wang, G.-M. Time-dependent creep and shrinkage analysis of curved steel–concrete composite box beams. *Mech. Adv. Mater. Struct.* **2021**. [CrossRef]

35. Su, R. Dynamic Response Analysis and Fatigue Reliability Study of Composite Box Girder Bridge-Train System Considering Time-Varying Effects. Master's Thesis, Beijing Jiaotong University, Beijing, China, 2022. (In Chinese)
36. Comite Euro International Du Beton. *CEB-FIP Model Code 1990*; Thomas Telford: London, UK, 1993.
37. Xia, H.; Roeck, G.D.; Goicolea, J.M. *Bridge Vibration and Controls: New Research*; Nova Science Publishers Inc.: New York, NY, USA, 2012.